Polymerization of Methyl Methacrylate Using Four-Coordinate (α-Diimine)iron Catalysts: Atom Transfer Radical Polymerization vs Catalytic Chain Transfer

Vernon C. Gibson,* Rachel K. O'Reilly, Duncan F. Wass, Andrew J. P. White, and David J. Williams

Department of Chemistry, Imperial College, Exhibition Road, South Kensington, London, UK SW7 2AY

Received January 15, 2003
Revised Manuscript Received March 6, 2003

Atom transfer radical polymerization (ATRP) is now well established as a highly versatile method for the synthesis of novel materials.[1,2] Following the pioneering contributions of Matyjaszewski[3] and Sawamoto[4] on copper and ruthenium systems, respectively, the range of catalysts has been extended to a number of other metals, including Fe,[5] Ni,[6] Pd,[7] and Rh.[8] Of these, iron offers particular attractions due to its biocompatibility,[9] which is especially relevant to the synthesis of materials for food packaging and in vivo applications.

We have been employing a ligand-oriented design approach for the development of new iron catalysts for olefin polymerization, especially ethylene polymerization. The most active and most widely applicable catalysts to date are based on ligands containing imine donors, especially tridentate bis(imino)pyridines.[10] In ATRP catalysis, unsaturated nitrogen donors have been investigated extensively for copper[1,11] but have received much less attention for iron-based systems. Studies by Matyjaszewski[12] on five-coordinate iron(II) complexes containing bis(imino)pyridines have suggested that these tridentate ligands have limited potential for Fe-based ATRP catalysts, most probably due to steric crowding within the metal coordination sphere. With a view to gaining a better understanding of the factors important for the stabilization of well-defined iron ATRP catalysts containing imine donors, we were attracted to a remarkably stable class of four-coordinate iron complex first described by Dieck and co-workers.[13] These complexes contain bidentate α-diimine ligands which stabilize a pseudotetrahedral coordination geometry. Inspection of space-filled models suggested that interconversion between four- and five-coordinate species may be better suited to ATRP catalysis where relatively large halogen atoms are transferred reversibly between the metal center and the end of the growing polymer chain. We have recently described a family of ATRP catalysts of type **1** (Scheme 1) and outlined their use for the polymerization of styrene.[14] Here we report our studies on the use of this catalyst system for the polymerization of methyl methacrylate (MMA) and the finding that alkylimino substituents favor ATRP while arylimines give rise to catalytic chain transfer (CCT).

The Fe(α-diimine)Cl_2 catalysts containing alkyl and aryl substituents are readily prepared by treatment of $FeCl_2$ with the appropriate α-diimine in diethyl ether. The molecular structure of the cyclohexyl derivative **1a** has been reported previously and shown to be mononuclear and pseudotetrahedral.[14] The results of MMA polymerizations using catalysts **1a**−**d** are collected in Table 1.[15] Employing ethyl 2-bromoisobutyrate (EBrB) as an initiator, MMA (100 equiv) polymerizes smoothly in the presence of **1a** in toluene (1:10 w/w ratio) at 80 °C to give narrow polydispersity PMMA (run 1). The semilogarithmic plot of $\ln([M]_0/[M])$ vs time is linear (up to conversions of 90%), with a pseudo-first-order rate constant (k_{obs}) of 0.13 h^{-1}, indicating that the radical concentration is constant throughout the polymerization run. Molecular weights (M_n) increase linearly with conversion and with monomer:initiator ratio; a plot of M_n vs monomer:initiator ratio is shown in Figure 1a. Halide analysis confirms the presence of one halogen per polymer chain,[16] and NMR spectroscopy shows a fully saturated product. The catalyst containing cyclododecyl substituents on the imine nitrogen donors (**1b**) affords a similarly controlled polymerization under ATRP conditions (run 2).

Polymerizations of MMA using the aryl derivatives **1c** and **1d** were examined under similar conditions (runs 3 and 4). However, in these cases the semilogarithmic plots of $\ln([M]_0/[M])$ vs time are nonlinear; the M_n of the resultant polymer samples do not increase linearly over time and are not in accord with the values calculated on the basis of monomer:initiator ratio. However, monomer conversion does increase in a semilinear manner with time, suggesting that a chain transfer mechanism is operating. Figure 1b compares plots of M_n vs conversion for catalysts **1a** and **1c**. While the alkylimine derivative **1a** gives a linear increase in M_n with conversion, polymerizations using **1c** generate low molecular weight PMMA with M_n independent of conversion. Halide microanalyses of polymer samples generated using **1c** show no halide content. Moreover, ^1H and ^{13}C NMR spectroscopic analyses reveal vinylidene end groups indicative of a β-hydrogen chain transfer process.

Scheme 1. Compounds 1a−1d

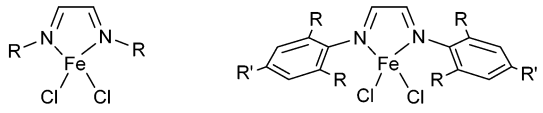

Table 1. Results of MMA Polymerizations at 80 °C Using Catalysts 1a−1d ([Catalyst] = 0.1 mM, [EBrB] = 0.1 mM, $[MMA]_0$ = 0.1 M, 1 g of Toluene)

run	catalyst	reaction time (h)	% conv	M_n(calc)	M_n	MWD
1	**1a**	2	13	1300	1700	1.34
	1a	6	49	4900	5400	1.30
	1a	14	84	8400	9000	1.21
2	**1b**	2	18	1800	2600	1.29
	1b	6	53	5300	6000	1.23
	1b	14	93	9300	10 200	1.18
3	**1c**	2	8	800	2700	1.56
	1c	6	31	3100	3800	1.59
	1c	14	78	7800	3600	1.49
4	**1d**	2	11	1100	2300	1.55
	1d	6	27	2700	2000	1.47
	1d	14	67	6700	2200	1.49

* Corresponding author: Tel 020 7594 5830; Fax 020 7594 5810; e-mail V.Gibson@ic.ac.uk.

10.1021/ma034046z CCC: $25.00
Published on Web 03/27/2003

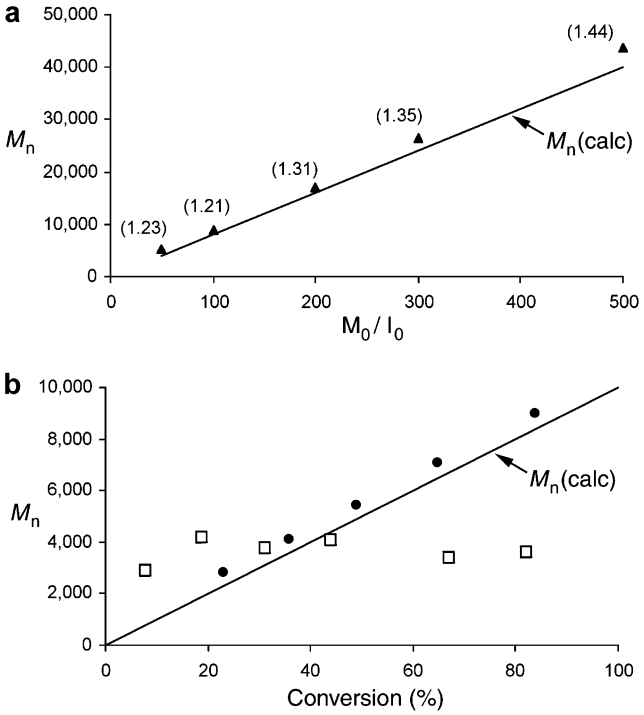

Figure 1. (a) Plot of molecular weight vs M_0/I_0 for catalyst **1a** with MWD in parentheses ([**1a**] = 0.1 mM, [EBrB] = 0.1 mM, $[MMA]_0$ = 0.5, 1.0, 2.0, 3.0, and 5.0 M, 10% w/w ratio toluene). (b) Plot of molecular weight vs conversion for complexes **1a** (●) and **1c** (□) ([catalyst] = 0.1 mM, [EBrB] = 0.1 mM, $[MMA]_0$ = 0.1 M, 1 g toluene, 80 °C).

To explore the possibility of a metal-based catalytic chain transfer mechanism, the catalyst concentration was increased 4-fold, whereupon the molecular weight decreased from 3600 Da (catalyst concentration 0.1 mM) to 1100 Da (catalyst concentration 0.4 mM). Further, if an AIBN-initiated polymerization is carried out in the presence of **1c** or **1d**, much reduced molecular weights are obtained. In the case of **1d**, the molecular weight is lowered from ca. 35 000 Da in the absence of the iron(II) complex to ca. 6000 Da when it is present.[17] These observations are consistent with the iron(II)−α-diimine complexes bearing aryl substituents acting as catalytic chain transfer reagents. In the case of styrene polymerization using **1c**,**d**, we were unable to rule out the possibility of an outer-sphere electron transfer (OSET) mechanism and offered an explanation for the poor ATRP performance of the aryldiimine catalysts on the basis of unfavorable electronic properties, as indicated by cyclic voltammetry measurements. We have since been able to obtain crystals of the 2,6-diisopropylphenyl derivative **1d**, which has provided an opportunity to examine the steric constraints around the iron center in closer detail.

Crystals of **1d** suitable for X-ray analysis were grown by slow diffusion of a dichloromethane solution of **1d** into an equal volume of heptane. The molecular structure is shown in Figure 2, and selected bond lengths and angles are collected in the figure caption. The structure showed the complex to have crystallographic C_s symmetry about a plane passing through the metal center and both chloride ligands and bisecting the C(1)−C(1′) bond. The bond lengths within the chelate ring are unexceptional and show the C=N bonds to have pronounced double-bond character [1.255(4) Å]. The geometry at the iron center is distorted tetrahedral [angles in the range 76.8(1)°−119.0(1)°] with the $FeCl_2$ and

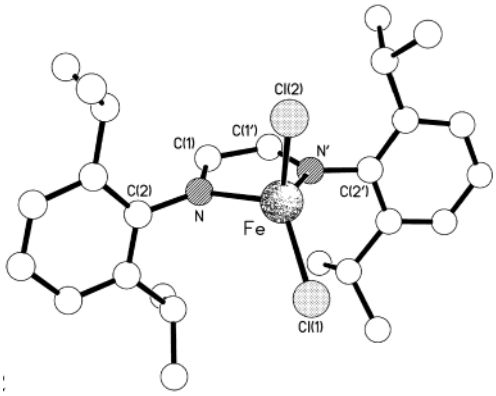

Figure 2. Molecular structure of **1d**. Selected bond lengths (Å) and angles (deg): Fe−N 2.108(3), Fe−Cl(1) 2.195(2), Fe−Cl(2) 2.222(2), N−C(1) 1.255(4), C(1)−C(1′) 1.478(6), N−Fe−N′ 76.84(14), N−Fe−Cl(1) 118.98(9), N−Fe−Cl(2) 108.30(8), Cl(1)−Fe−Cl(2) 118.17(7).

FeN_2 planes being perfectly orthogonal to each other. The chelate ring is folded about the N···N vector by ca. 20°, the iron atom lying 0.58 Å out of the C_2N_2 plane (which is perfectly flat as a consequence of the C_s symmetry) in the direction of Cl(2). This gives rise to a distinct axial/equatorial disposition of the two chloride ligands [Cl(2) "axial" and Cl(1) "equatorial"] with a consequent effect on their Fe−Cl distances with that to Cl(2) being noticeably longer [at 2.222(2) Å] than that to Cl(1) [2.195(2) Å]. The folding of the chelate ring also causes the two 2,6-diisopropylphenyl rings to be bent out of the C_2N_2 plane [away from Cl(2)] such that their Ar−N bonds are inclined to each other by ca. 161°. The planes of the 2,6-diisopropylphenyl rings are tilted with respect to the C_2N_2 plane by ca. 78°, but they are almost orthogonally disposed with respect to the FeN_2 plane (86°). There are no intermolecular packing interactions of note.

The conformation adopted by the bis(2,6-diisopropylphenyl) species **1d** contrasts with that of its bis(cyclohexyl) analogue **1a** recently reported by ourselves.[14] In the crystal structure of **1a** the iron atom is coplanar with the chelate ring (unlike in **1d**, vide supra), and the two N−C bonds to the cyclohexyl substituents are thus very nearly coplanar with the chelate ring, giving rise to an open geometry around the metal center (Figure 3a). The folded chelate plane in **1d**, however, with its associated bending of the two N−Ar bonds out of the C_2N_2 plane and the tilting of the 2,6-diisopropylphenyl rings with respect to this plane, causes significant steric crowding "beneath" the iron center (Figure 3b); the isopropyl methine carbon···isopropyl methine carbon separations "above" and "below" the metal center are 6.39 and 4.30 Å, respectively.

Thus, in conclusion, a comparison of space-filled views for **1d** and its cyclohexyl analogue **1a** (Figure 3) show that the iron center is relatively accessible in the case of the **1a**, but less so in the case of **1d**. This may lead to higher energetic barriers to accommodating a halogen atom at the metal centers of the more sterically hindered aryl derivatives **1c** and **1d** and thus may have an important bearing on allowing a competitive β-hydrogen chain transfer pathway to dominate.

Crystal data for **1d**: $C_{26}H_{36}N_2Cl_2Fe$, M = 503.3, orthorhombic, *Pnma* (no. 62), a = 12.231(1), b = 21.664(1), c = 10.378(3) Å, V = 2749.8(8) Å^3, Z = 4 (C_s symmetry), D_c = 1.216 g cm^{-3}, μ(Cu Kα) = 6.28 mm^{-1}, T = 293 K, dark green prisms; 2209 independent measured reflec-

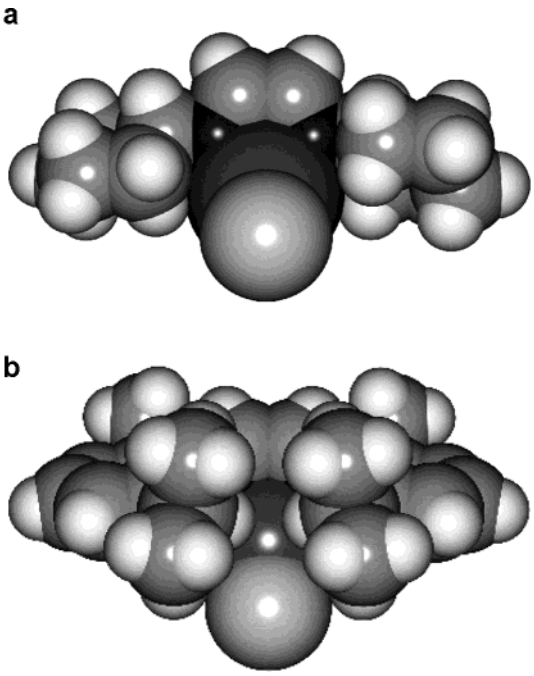

Figure 3. Comparative space-filling representations of the structures of complex **1a** (a) and complex **1d** (b).

tions, F^2 refinement, $R_1 = 0.056$, $wR_2 = 0.146$, 1723 independent observed absorption corrected reflections [$|F_o| > 4\sigma(|F_o|)$, $2\theta \leq 124°$], 146 parameters.

Acknowledgment. BP Chemicals Ltd. is thanked for financial support (R.K.O'R.). Prof. K. Matyjaszewski and Dr. D. J. Irvine (ICI, Uniqema) are thanked for helpful discussions and Dr. Jane Boyle for assistance with NMR measurements.

References and Notes

(1) Matyjaszewski, K.; Xia, J. *Chem. Rev.* **2001**, *101*, 2921−2990.
(2) Kamigaito, M.; Ando, T.; Sawamoto, M. *Chem. Rev.* **2001**, *101*, 3689−3745.
(3) Wang, J. S.; Matyjaszewski, K. *J. Am. Chem. Soc.* **1995**, *117*, 5614−5615.
(4) Kato, M.; Kamigaito, M.; Sawamoto, M.; Higashimura, T. *Macromolecules* **1995**, *28*, 1721−1723.
(5) Ando, T.; Kamigaito, M.; Sawamoto, M. *Macromolecules* **1997**, *30*, 4507−4509. Matyjaszewski, K.; Wei, M.; Xia, J.; McDermott, N. E. *Macromolecules* **1997**, *30*, 8161−8164. Takahashi, H.; Ando, T.; Kamigaito, M.; Sawamoto, M. *Macromolecules* **1999**, *32*, 3820−3823. Kotani, Y.; Kamigaito, M.; Sawamoto, M. *Macromolecules* **1999**, *32*, 6877−6880. Teodrescu, M.; Gaynor, S. G.; Matyjaszewski, K. *Macromolecules* **2000**, *33*, 2335−2339. Louis, J.; Grubbs, R. H. *Chem. Commun.* **2000**, 1479−1480. Kotani, Y.; Kamigaito, M.; Sawamoto, M. *Macromolecules* **2000**, *33*, 3543−3549.
(6) Granel, C.; Dubois, P.; Teyssié, P.; Jêromé, R. *Macromolecules* **1996**, *29*, 8576−8582. Uegaki, H.; Kotani, K.; Kamigaito, M.; Sawamoto, M. *Macromolecules* **1997**, *30*, 2249−2253.
(7) Lêcomte, P.; Drapier, I.; Dubois, P.; Teyssié, P.; Jêromé, R. *Macromolecules* **1997**, *30*, 7631−7633.
(8) Lêcomte, P.; Drapier, I.; Dubois, P.; Teyssié, P.; Jêromé, R. *Macromolecules* **1998**, *31*, 542−544.
(9) See: The Biological Chemistry of Iron. In *Proceedings of the NATO Advanced Study Institute, Edmonton, Alberta, Canada, 1981*; Dunford, H. B., Dolphin, D., Raymond, K. N., Sieker, L., Eds.; D. Reidel Publishing Co.: Dordrecht, 1981.
(10) (a) Britovsek, G. J. P.; Gibson, V. C.; Kimberley, B. S.; Maddox, P. J.; McTavish, S. J.; Solan, G. S.; White, A. J. P.; Williams, D. J. *Chem. Commun.* **1998**, 849−850. (b) Small, B. L.; Brookhart, M.; Bennett, A. M. A. *J. Am. Chem. Soc.* **1998**, *120*, 4049−4050.
(11) Haddleton, D. M.; Jasieczek, C. B.; Hannon, M. J.; Shooter, A. J. *Macromolecules* **1997**, *30*, 2190−2191.
(12) Göbelt, B.; Matyjaszewski, K. *Macromol. Chem. Phys.* **2000**, *201*, 1619−1624.
(13) Dieck, H. T.; Diercks, R. *Angew. Chem.* **1983**, *95*, 801−802.
(14) Gibson, V. C.; O'Reilly, R. K.; Reed, W.; Wass, D. F.; White, A. J. P.; Williams, D. J. *Chem. Commun.* **2002**, 1850−1851.
(15) Polymerizations were performed under an inert atmosphere in a 15 cm^3 glass ampule fitted with a Teflon stopcock. The ampule was equipped with a magnetic stirrer bar, and the following were placed in it in the order: monomer, initiator, catalyst, and solvent in a 100:1:1:10 ratio. Then the ampule was sealed. In all cases the catalyst was soluble in the monomer solution. The ampules were transferred to a preheated oil bath at 80 °C. After magnetic stirring for the allotted period of time an aliquot (0.1 mL) was removed and quenched by addition of THF (1 mL). Conversion was determined by integration of monomer (2.5 and 6.3 ppm) vs polymer backbone (0.7−1.4 ppm) resonances in the ^1H NMR spectrum of the crude product (in $CDCl_3$). The polymer was purified by redissolving in THF (5 mL) and precipitating from a rapidly stirred acidified (5%) methanol solution. GPC chromatograms were recorded on a Knauer differential refractometer connected to a Gynotek HPLC pump (model 300) and two PSS columns (pore size 10 μm) at a flow rate of 1.00 cm^3 min^{-1} using $CHCl_3$ as the eluent. The columns were calibrated against poly(methyl methacrylate) standards with molecular weights ranging from 940 to 174 000. Samples were filtered through a 0.45 μm filter immediately prior to injection. Analysis was performed using Version 3.0 of the Conventional Calibration module of the Viscotek SEC^3 software package.
(16) Microanalysis for poly(methyl methacrylate) produced using **1a**, $M_n = 5400$, % halide, found (calcd) 1.39 (1.48).
(17) Polymerizations were performed as described previously in bulk at 110 °C. The ratio of monomer to initiator to catalyst (**1d**) was 100:0.625:1 and 100:0.625:0. For catalyst **1a**, under identical conditions, no decrease in molecular weight was observed.

MA034046Z